JMJD3 is a Key Regulator of Dopamine Synthesis in Ventral Tegmental Area Dopamine Neurons.

Running title: JMJD3 activates TH and regulates VTA DA synthesis.

Xi-Biao He[1,*], Fang Guo[1,#], Wei Zhang[2,#], Yi Wu[1,#], Weidong Le[3], Hui-Jing Wang[4], Qinming Zhou[5], Haozhi Huang[1]

[1] Laboratory of Stem Cell Biology and Epigenetics, School of Basic Medical Sciences, Shanghai University of Medicine and Health Sciences, Shanghai 201318, China.

[2] State Key Laboratory of Microbial Metabolism, School of Life Science and Biotechnology, Shanghai Jiao Tong University, Shanghai 200240, China

[3] Center for Translational Medicine, Shanghai University of Medicine & Health Sciences, Shanghai, People's Republic of China.

[4] Laboratory of Neuropsychopharmacology, School of Basic Medical Sciences, Shanghai University of Medicine and Health Sciences, Shanghai 201318, China

[5] Department of Neurology, Ruijin Hospital, Shanghai Jiao Tong University School of Medicine, Shanghai 200025, China

# These authors contribute equally to this work.

* Corresponding author

Xi-Biao He

Address: 279 Zhouzhu Highway, Pudong New Area, Shanghai, 201318, China

Tel: 86-18516097628

E-mail: hexb@sumhs.edu.cn

Abstract

Regulation of dopamine (DA) biosynthesis is critical for the functionalities of midbrain DA neurons. Tyrosine hydroxylase (TH) is the rate-limiting enzyme for dopamine (DA) biosynthesis in midbrain DA neurons. Here we report that DA contents are decreased in the midbrain and striatum of DA neuron-specific JMJD3 conditional knockdown mice. Consistent results are obtained from mice underwent pharmaceutical JMJD3 inhibition. Biochemical and histological experiments reveal that TH mRNA and protein levels are specifically decreased in DA neurons residing in ventral tegmental area but not substantia nigra pars compacta. On behavioral level, JMJD3 knockdown affects inflammation-induced chronic mechanical hyperalgesia but not locomotor coordination, corresponding to DA-associated behavior in ventral tegmental area and in substantia nigra pars compacta, respectively. Mechanistically, using a midbrain DA neuron culture, we demonstrate that JMJD3 transactivates TH gene expression through direct binding onto TH promoter and catalyzing H3K27 de-methylation. In summary, our findings reveal a novel role of JMJD3 in adult midbrain DA system and suggest its functional specificity with DA subtype heterogeneity.

Key words: dopamine neuron; JMJD3; tyrosine hydroxylase; chronic pain; ventral tegmental area

Introduction

Dysregulation of dopamine (DA) system in the brain has been implicated in a number of neurological and psychiatric diseases [1, 2]. As the major DA producer in central nervous system (CNS), midbrain DA neurons are anatomically composed of three nuclei, including the retrorubral field, the substantia nigra pars compacta (SNpc) and ventral tegmental area (VTA). SNpc DA neurons primarily project into dorsal striatum via mesostriatal pathway and regulate voluntary movement control, loss of which is associated with locomotor dysfunction in Parkinson's disease (PD). By contrast, VTA DA neurons primarily project into ventral striatum/nucleus accumbens and prefrontral cortex via mesolimbic and mesocortical pathways, regulating a wide variety of cognition-related behaviors such as emotion, reward and addiction [3, 4]. In addition, the involvement of midbrain DA transmission in the central regulation of pain is well recognized [5–10]. In particular, inflammatory stimuli have been reported to directly down-regulate VTA DA activity and inhibit mesolimbic pathway, indicating VTA DA neurons as a major mediator of chronic pain [11–13]. However, the molecular mechanisms underlying this association remain largely unclear.

Tyrosine hydroxylase (TH) catalyzes the conversion of L-tyrosine to L-dihydroxyphelalanine (L-DOPA), which is the rate-limiting step for a series of catecholamine biosynthesis including DA, epinephrine and norepinephrine (NE). In CNS, TH is mainly expressed in neurons distributed in midbrain, hypothalamus, olfactory bulb and retina, yet only midbrain TH-expressing neurons are major DA producers [4]. Gene knockout studies have demonstrated that TH-mediated catecholamine synthesis is essential for fetal brain development and postnatal survival [14, 15], and mutation-induced TH deficiency causes a neurological disorder that is mostly treatable by L-DOPA [16]. Moreover, downregulation of TH activity has been reported in surviving but dysfunctional midbrain DA neurons in PD and pathological aging [17], demonstrating pathophysiological effects of TH expression change on midbrain DA functions. Depending on context, TH expression and activity are epigenetically, transcriptionally and post-translationally regulated [18]. Despite of a large number of transcription factors identified [19–25], the roles of

epigenetic regulators in the transcriptional control of TH in adult midbrain DA neurons are just beginning to get revealed.

Jumonji C-domain-containing histone deacetylase 3 (JMJD3) is a histone deacetylase specifically demethylating histone 3 lysine 27 (H3K27), which is in general related with a chromatin structure remodeling resulting in a transcriptional regulation from repression to activation [26]. This epigenetic regulator is widely involved in various biological functions of cells, including early embryonic development [27–30], neural commitment [31, 32], reprogramming [33], epidermal differentiation [34], inflammation [35–39], cellular senescence [40] and bone formation [41–43]. We have previously shown that JMJD3 plays a key role in determining TH expression in midbrain DA neural precursor cells (NPCs), facilitating their differentiation into DA neurons [44]. JMJD3-induced H3K27 demethylation of TH promoter in DA NPCs is a prerequisite for the binding of other DA fate master regulators and transcriptional initiation. Besides that, little is known about the role of JMJD3 in DA system, in particular in mature DA neurons after differentiation.

In this study, we ask the question about how the DA neuron-specific knockdown of JMJD3 affects the TH expression and DA biosynthesis across various brain regions in adult mice. Furthermore, we provide evidence for the potential correlation of region-specific alterations of DA level with their behavioral consequences, highlighting a critical role of VTA DA neuron-specific JMJD3 in the regulation of chronic pain.

Materials and Methods

Ethics

All animal experiments were approved by the animal ethics committee of Shanghai University of Medicine and Health Sciences and have been performed in accordance with the ethical standards laid down in the 1964 Declaration of Helsinki and its later amendments.

Animals

For pharmaceutical JMJD3 inhibition experiments, 4-month-old male C57BL/6 mice were purchased from Shanghai Jiesijie Experimental Animal Co. GSK-J4 dissolved in dimethyl sulfoxide (DMSO) was daily injected intraperitoneally at 20 mg/kg body weight into mice for five consecutive days. In parallel, DMSO was injected in the same manner as a negative control. For TH-specific JMJD3 knockdown experiments, TH-Cre transgenic mice (a kind gift from Dr. Weidong Le) were crossbred with heterozygous floxed JMJD3 mice (a kind gift from Dr. Degui Charlie Chen) to generate TH-specific JMJD3 conditional knockdown mice, whereas littermates of TH-Cre mice were used as control mice. All animals were housed under standard conditions with controlled 12-hour light/dark cycles with food and water provided ad libitum.

Cell culture

Primary midbrain DA neurons were cultured as previously described [44] with minor modifications. Briefly, neural precursor cells extracted from embryonic day 11 mouse ventral mesencephalon were mechanically dissociated into single cells and plated onto 24-well plates or 6-well dishes precoated with 15 μg/ml poly-L-ornithine and 1 μg/ml fibronectin. Cells were cultured in serum-free Neurobasal media supplemented with N2 and B27 supplements and 1% Penecillin/Streptomycin for 7 days to reach a complete DA neuronal differentiation. After that, GSK-J4 or DMSO were treated for 24 hours. MES23.5 cells were cultured in DMEM supplemented with 2% fetal bovine serum and 1% Penecillin/Streptomycin. All cells were incubated in 5% CO2, 37 °C incubator.

Real-time PCR analysis

RNAs were extracted from cultured cells and tissues using RNA extraction kit and reverse transcribed into cDNAs (both from TAKARA) according manufacturers' instructions. Real-time PCR was performed on a Real time system (Roche) using SYBR green supermix (Vazyme). The comparative cycle threshold method was used for quantification. Gene expression values were normalized to those of Gapdh. The primers are listed in Supplementary Table S1A.

Fluorescence immunostaining analysis

Brain tissues were pre-fixed with 4% paraformaldehyde by cardiac perfusion and post-fixed for 1 hour, dehydrated in 30% sucrose and stored in embedding compound (Tissue-Tek) at -70°C until cryosection. Tissues were cryosectioned into 14 μm thickness (Leica CM1950). Cultured cells were fixed with 4% paraformaldehyde for 20 mins. For immunostaining, tissue slices or cultured cells were permeabilized and blocked with PBS with 0.3% TritonX-100 and 1% bovine serum albumin for 40 mins, incubated with mouse anti-TH primary antibody (Sigma) diluted with blocking solution at 4□ overnight. Alexa Fluor series of second antibodies (Thermo Scientific) were applied for one hour at room temperature. Cells were finally counterstained with 4',6-diamidino-2-phenylindole (DAPI) and examined using fluorescence microscope (Leica DMi8).

HPLC-MS analysis

HPLC-MS experiments were performed as previously described [45, 46]. Briefly, samples from different brain regions after mouse sacrifice were homogenized in ice-cold 0.2M perchloric acid/methanol, sonicated (Bioruptor) and centrifuged at 10000 g for 20 min. Supernatants were then filtered through 0.22 μm filter and stored in -80□. At least four animals per genotype or drug treatment were used. Analytes were separated using a Model 1260 HPLC system consisting of a binary pump, on-line degasser, thermostated dual 54-well plate autosampler, and a thermosated column compartment (Agilent Technologies, Santa Clara, CA) with a Poroshell 120 SB-C18 reverse phase column (3.0x100 mm, 2.7 μm, particle size, Agilent Technologies, Santa Clara, CA) temperature-controlled at 25 □. The mobile phase consisted of A (1mM ammonium formate, 0.1%(v/v) formic acid and 1%(v/v) methanol in water) and B (1 mM ammonium formate 0.1%(v/v) formic acid and 0.9%(v/v) H2O in methanol). The gradient conditions of the mobile

phase were as follows: 0 min, 5% B; 20 min,95% B; 21 min, 5% B and 28 min, 5% B. The flow rate of the mobile phase was 0.3 ml/min, and the injection volume was 10μl. For MS analysis, LC flow was coupled to an Agilent model 6470 triple quadrupole (QqQ) MS (Agilent Technologies, Santa Clara, CA), equipped with an Agilent Jet Stream (AJS) electrospray ionization (ESI) source. The mass spectrometer was operated with the following parameters: capillary voltage, 4000 V for positive and 3500 V for negative; nozzle voltage, 500 V. Nitrogen was used as the drying (5 L/min, 300 ℃), sheath (11 L/min, 250 ℃) and nebulizer gas (45 psi). The data was acquired using Agilent MassHunter Workstation Data Acquisition Software (revision B.04). Multiple-reaction-monitoring transitions parameters, such as precursor ions, product ions, fragmentor voltage, collision energy (CE) as well as polarity were shown in Supplemental Table S1. For the compounds which had two product ions, it was shown that the product ion was used as quantitative ion or qualitative one in Supplemental Table S1B. The dwell time was 50 ms for transitions.

Mechanical hyperalgesia test

Complete Freund's adjuvant (CFA)-induced chronic mechanical hyperalgesia was assessed as previously described [47]. Briefly, baseline responses were measured using von Frey hairs (bending force range from 0.02-1.4 g, starting with 0.16g; Stoelting) after mice were placed on a wire grid without receiving any nociceptive stimulation for 2 hours. Next day, 20 μl CFA (Sigma-Aldrich) was injected intraplantarly, and the hyperalgesia responses were measured for various time points within 18 days.

The hair force was increased or decreased according to the response, and the 50% paw withdrawal threshold was calculated using the up and-down method [48]. Nociceptive responses include clear paw withdrawal, shaking, and licking. Stimulus and measurement were repeated if ambiguous responses such as ambulation occurred.

Hargreaves test

Thermal algesia to noxious stimulus was measured using a hot/cold plate analgesia meter for mice

(IITC) according to manufacturer's instructions. mice were put on a glass plate and the hind paw plantar surface was exposed to a beam of radiant heat (intensity latency 8-12 s) according to the Hargreaves method [49]. Latencies of hind paw withdrawal were recorded. The heat stimulation was repeated 2 times at an interval of 5 min for each mouse and the mean of both paws was calculated.

Grip strength test

Hindlimb grip strength was measured with a grip strength meter for mice consisted of a T-shaped metal bar connected to a force transducer (IITC). Briefly, mice were held by tails allowing them to grasp the metal bar with hind paws, followed by a pulling of the mice backwards by the tail until grip was lost. The peak force was automatically recorded in grams (g) by the device. The measurement of grip strength was repeated 5 times at an interval of 5 min for each mouse and the mean was calculated.

Accelerating rotarod test

The test was performed on a rotarod apparatus (IITC) according to manufacturer's manual. The 3 cm-diameter suspended rod was set to accelerate at a constant rate from 5 to 45 rpm in 240 s. Mice were pre-trained for 2 consecutive days before first trial. At each trial, mice were placed on the rod for a session of two repeats, with 180 s resting time allowed in between. A trial ended when the mouse fell off the rotarod or after reaching 240 s. The falling time was recorded and averaged of two repeats. Total four trials were performed for four consecutive days.

Cell counting and statistics

For in vivo analysis, at least 50 TH-immunoreactive or DAPI-stained cells were counted in each brain region for one animal. Data were derived from three mouse brains of same experimental group and expressed as mean ± S.E.M. For in vitro analysis, cultured cells were counted in at least 10 random regions of each culture coverslip using an eyepiece grid at a magnification of 200 or 400X. Data are expressed as mean ± S.E.M. of three independent cultures. For HPLC-MS analysis, data were derived from four to seven mouse brains of same transgenic background and

expressed as mean ± S.E.M. Statistical comparisons were made using Student's t-test, one-way ANOVA with Tukey's post hoc analysis and two-way ANOVA with Sidak's multiple comparisons test (Graphpad Prism).

Results

JMJD3 deficiency causes decrease of DA level in mouse midbrain.

To investigate the effect of JMJD3 inhibition on aminergic neurotransmitters in the brain, a brain-penetrating JMJD3 inhibitor GSK-J4 [50] was daily injected intraperitoneally into adult male mice for five days and the contents of DA, NE, serotonin (5-HT) from different brain regions were examined by high performance liquid chromatography-mass spectrometry (HPLC-MS) analysis. The brain regions examined include frontal cortex, striatum, midbrain, cerebellum and medulla oblongata, where reside aminergic neurons and projections to different extents. We found that GSK-J4 caused significant decrease of DA content in striatum and midbrain but not in frontal cortex, cerebellum or medulla oblongata (Fig. 1A). By contrast, the content of NE was not altered in any brain regions (Fig. 1B), suggesting that the GSK-J4 effect on catecholamine was limited in DA system. However, of note, the level of 5-HT in cerebellum and medulla oblongata also underwent a significant decrease by GSK-J4 (Fig. 1C), indicating a wider range of effect on neurotransmitter by GSK-J4 in the brain.

Given the region specificity of DA level change, we hypothesized that JMJD3 inhibition in TH-expressing midbrain DA neurons contributed to the GSK-J4-induced decrease of DA content. To validate this, we constructed conditional JMJD3 knockdown (TH-KD) mice by crossbreeding transgenic mice carrying *Th*-CRE and loxP-floxed Jmjd3 loci. Knockdown of JMJD3 was confirmed by genotyping analysis (Suppl Fig. 1). We then measured the levels of DA, NE, 5-HT in different brain regions of TH-CRE and TH-KD mice by HPLC-MS. To exclude the sex heterogeneity, data from male and female mice were analyzed individually. The results demonstrated that the levels of DA in striatum and midbrain of TH-KD mice were significantly lower than those of TH-CRE mice in both sexes, whereas no significant difference was observed in frontal cortex, cerebellum and brainstem (Fig. 1D and Suppl Fig. 2A). Consistent results were also observed in the case of NE and 5-HT (Fig. 1E, F and Suppl Fig. 2B, C). Taken together, in vivo results from two different animal models provide compelling evidence indicating that the DA level is sensitive to JMJD3 activity in adult mouse midbrain DA neurons.

TH expression is specifically suppressed in VTA DA neurons.

The biochemical findings above suggested that the DA biosynthesis in midbrain DA neurons might be affected by JMJD3 activity. Therefore, we compared the mRNA expression of TH in TH-CRE and TH-KD mice. Conditional knockdown of JMJD3 caused remarkable decrease of mRNA levels of JMJD3 and TH in midbrain and striatum, but not in other brain regions (Fig. 2A). Consistently, immunofluorescence microscopy analysis showed that DA neurons in VTA exhibited remarkably lower TH immunoreactive intensity in TH-KD mice. By contrast, those in SNpc appeared to maintain the TH immunoreactive intensity (Fig. 2B, C). Importantly, the region-specific decrease of TH immunoreactive intensity correlated with the decrease of TH+ DA neuronal cell number (Fig. 2D). However, this did not reflect a loss of DA neurons but rather a disappearance of TH expression, as neither the total cell number nor the overall morphology in VTA was altered (data not shown). Collectively, these results suggest that down-regulation of TH transcription in DA neurons from midbrain, particularly from VTA, rather than loss of any of those cells, underlie JMJD3 inhibition-induced DA content decrease in mouse brain.

Mechanical hyperalgesia but not locomotor coordination is affected by JMJD3 knockdown.

Given the subtype heterogeneity of midbrain DA neurons, we assumed that DA levels are differentially down-regulated Next we asked

The results above suggest that JMJD3 determines the subtype heterogeneity of midbrain DA neurons. To confirm this, we investigated the behavioral outcomes of two DA-associated behavior tests that, according to previous studies, correspond to DA neuron functions in VTA and SNpc, respectively. For DA-associated behavior in VTA, we assessed the chronic inflammation-induced mechanical hyperalgesia in TH-CRE and TH-KD mice underwent Complete Freund's adjuvant (CFA)-induced chronic inflammatory pain [47, 51], whereas for DA-associated behavior in SNpc, locomotor coordination and motor skill learning were assessed by accelerating rotarod test [52–54]. Moreover, as DA levels differ along age and sex, mice were sub-grouped into male and female, young (4-6 months old (mo)) and old (12-14 mo).

As shown in Fig. 3A, intraplantar injection of CFA induced significant mechanical hyperalgesia within 3 hours in both TH-CRE and TH-KD young male mice. The hyperalgesia was not attenuated until the eighth day (D8) in TH-CRE mice, followed by a nearly complete recovery from D13, confirming the efficiency of this chronic inflammatory pain model. By contrast, the hyperalgesia lasted for at least 13 days in TH-KD mice, and was only slightly attenuated at D18, suggesting a remarkably extended period of chronic pain induced by TH-specific JMJD3 knockdown. Similar alterations were observed in young female mice (Fig. 3B). On the contrary, in old TH-CRE male mice, the chronic hyperalgesia was not attenuated even after 18 days of CFA injection (Fig. 3C), suggesting a critical role of aging in chronic inflammatory pain. In parallel, old TH-KD male mice also exhibited an extended period of hyperalgesia. Interestingly, the effect of aging on chronic pain was also evident in old TH-CRE female mice, but was much milder than that in old male ones. However, the chronic hyperalgesia was persisted for at least 13 days in old TH-KD female mice (Fig. 3D). To confirm the pain specificity, the thermal hyperalgesia was measured in parallel to mechanical hyperalgesia using a Hargreaves method [49] and no difference was observed (Suppl Fig. 3A). Collectively, these results demonstrated that, despite of the aging effect in wildtype, TH-specific knockdown of JMJD3 consistently caused extension of mechanical hyperalgesia regardless of age and sex, suggesting a direct association between JMJD3 and chronic inflammatory pain.

The accelerating rotarod test is often used to measure locomotor coordination in rodents. In addition, the accelerating rotarod test was performed for four consecutive days to enable a further demonstration of motor skill learning, which more likely reflects the vulnerability of DA depletion as previously reported [52, 55]. As expected, a decrease of locomotor activity was noticed in aged male mice of both groups in comparison to young male ones as previously reported [56], validating the specificity of the test. However, no significant difference of falling latency was found between TH-CRE and TH-KD mice within four trials, regardless of sex and age (Fig. 3E-H), suggesting that the locomotor function in mouse is not affected by JMJD3 defect in TH-expressing cells. In addition, no difference of grip strength was found between TH-CRE and TH-

KD mice regardless of sex and age (Suppl Fig. 3B), confirming that no interference was caused by defects in limb muscle strength.

JMJD3 directly transactivates *Th* gene.

To investigate the molecular mechanism underlying JMJD3-mediated *Th* gene expression in DA neurons, we recruited a well-established primary midbrain DA neuron culture derived from embryonic day 11 mouse ventral mesencephalon [44, 57, 58]. At this stage, the SNpc and VTA and their projecting pathways are not anatomically or molecularly distinct [59, 60], enabling an in vitro culture of DA NPCs with differentiation potential into both DA subtypes. The cells were maintained in a modified Neurobasal medium without any mitogens for 6 days to guarantee a complete differentiation of post-mitotic DA neurons. After that, GSK-J4 was treated for 1 day to investigate its effect on TH expression. A dose-dependent decrease of TH-expressing cells was observed (Fig. 4A), together with a down-regulation of *Th* gene expression (Fig. 4B). Similar results were seen in GSK-J4-treated MES23.5 cells [61], a widely-used DA neuronal hybrid cell line consistently expressing TH (Suppl Fig. 4). To confirm the specificity of GSK-J4, we performed short hairpin RNA-mediated JMJD3 knockdown (sh-JMJD3) in primary DA neuron culture and observed similar results (Fig. 4C, D). These results demonstrate that JMJD3 is a positive regulator for *Th* gene expression and TH activity in midbrain DA neurons.

As a chromatin modifier, JMJD3 can bind to DNA and specifically demethylate H3K27 tri-methylation. Using chromatin immunoprecipitation (ChIP) assay, we found that GSK-J4 induced region-specific H3K27 tri-methylations within 1 kilo bp of *Th* gene promoter (Fig. 4E). Moreover, JMJD3 was specifically enriched within -750 to -450 bp of *Th* promoter, and its enrichment was remarkably decreased after GSK-J4 treatment (Fig. 4F). These results indicated that JMJD3 participated in transactivation of *Th* gene through direct binding and erasing the repressive histone modification mark on *Th* promoter in DA neurons.

Discussion

We report here for the first time a novel role of JMJD3 in the maintenance of DA level in adult mouse midbrain, suggesting JMJD3 as a critical regulator for DA-associated neural circuits and behaviors. Moreover, we have identified the transcription and histone modification status of TH gene as the mechanistic targets of JMJD3, indicating reduced DA biosynthesis as a direct consequence of JMJD3 inhibition. Indeed, the DA levels are mostly affected in midbrain and striatum, likely due to their specific co-expression of aromatic L-amino acid decarboxylase, another enzyme essential for the production of DA besides TH [4]. Importantly, midbrain DA neurons are not lost by DA neuron-specific JMJD3 knockdown, demonstrating a non-cell toxic suppression of TH and reduction of DA content, which is largely distinguished from the neurotoxic cause commonly found in PD [62].

Given the diverse molecular signature, synaptic inputs and functionality between DA neurons in VTA and SNpc [63, 64], the DA subtype-specific effect of JMJD3 is not surprising. The behavioral outcome of rotarod test is consistent with the immunohistology result of no difference of TH expression in SNpc DA neurons. This finding also suggests that the decrease of DA level in midbrain DA neurons and the striatum they projected into, consistently by genetic JMJD3 knockdown or likely temporally by GSK-J4, does not primarily come from SNpc and is not directly associated with locomotor dysfunction. By contrast, DA neurons in VTA innervating into the ventral striatum are likely to be the major victim suffering decrease of DA. Indeed, DA neurons in VTA of TH-KD mice suffered significantly more loss of TH immunoreactive intensity than those in SNpc. This distinct sensitivity to JMJD3 activity between VTA and SNpc midbrain DA neurons deserves a comprehensive investigation in the future.

A high consistency of neurotransmitter content changes is observed between drug-induced global JMJD3 inhibition and DA neuron-specific JMJD3 knockdown. Results from both animal models demonstrate that the JMJD3 effect on catecholamine contents is limited to DA, as the contents of NE are not altered in either model. Interestingly, remarkable reductions of 5-HT contents are detected in the cerebellum and medulla oblongata from both animal models. It is unknown

whether this is due to direct intracellular regulation of 5-HT neurons in cerebellum and/or medulla oblongata, or indirectly from DA pathways. However, it is less likely that the 5-HT level is regulated in a similar manner as the DA level, i.e., through transcriptional repression of tryptophan hydroxylase, the rate limiting enzyme for 5-HT, as treating primary 5-HT neuron cell culture with GSK-J4 did not decrease mRNA or protein levels of tryptophan hydroxylase (data not shown). It is also intriguing to ask to what extent does the alteration of 5-HT level in these regions contribute to the behavioral changes observed in TH-KD mice.

A large number of studies have described the involvement of mesolimbic DA system in nociception and neuropathic pain [5, 8, 11, 64–76]. In particular, DA contents in striatum and VTA DA neurons are negatively correlated with mechanical hyperalgesia in various mouse models of neuropathic pain [65–69, 77]. Evidence also exist suggesting that TH-expressing cells from other CNS regions, such as A11 hypothalamic DA neurons innervating the spinal cord and dorsal root ganglion neurons expressing C-low threshold mechanoreceptors as potential players in the descending pain modulation [70, 78–80]. However, we found that there was no significant difference of the DA level in hypothalamus between TH-CRE and TH-KD mice (data not shown), and JMJD3 expression is almost undetected in TH-expressing dorsal root ganglion neurons (unpublished data). Therefore, we conclude that the contributions of these regions to JMJD3-related hyperalgesia, if any at all, are not comparable to that of VTA DA neurons and mesolimbic DA system.

JMJD3 is a common epigenetic modifier involved in various cellular functions, inhibition of which has shown promising potential in cancer therapy. JMJD3 inhibitor GSK-J4 has recently been suggested as an efficient epigenetic targeted therapy for pediatric brainstem glioma and high-risk neuroblastoma [81, 82]. Of note, we showed that intraperitoneal injection of GSK-J4 into adult mice for 5 days would have remarkable impact on the metabolism of DA system in brain. Our finding raises concerns about the adverse effects of this drug on DA-related behaviors, and proposes a closer look into these effects in pre-clinical and clinical trials with JMJD3 as therapeutic target.

Acknowledgements

We thank Dr. Weidong Le and Dr. Degui Charlie Chen for providing TH-CRE and JMJD3 loxP mice. X.B.H. is supported by the National Natural Science Foundation of China (31701287). F.G. is supported by the National Natural Science Foundation of China (32100779).

Author Contributions

X.B.H. conceived the study, performed the experiments, generated figures and wrote the paper. W.Z. performed HPLC-MS work and drafted the manuscript. Y.W. performed the experiments, generated figures and drafted the manuscript. F.G., H.H. performed the experiments. Q.Z. helped generate the mouse models. H.J.W. provided technical support for pain-related experiments. All authors have approved the final version of the manuscript.

Conflict of Interest

The authors declare no competing interests.

Reference

1. Iversen SD, Iversen LL. Dopamine: 50 years in perspective. Trends in Neurosciences. 2007;30:188–193.
2. Grace AA. Dysregulation of the dopamine system in the pathophysiology of schizophrenia and depression. Nat Rev Neurosci. 2016;17:524–532.
3. Luo SX, Huang EJ. Dopaminergic Neurons and Brain Reward Pathways. The American Journal of Pathology. 2016;186:478–488.
4. Björklund A, Dunnett SB. Dopamine neuron systems in the brain: an update. Trends in Neurosciences. 2007;30:194–202.
5. Scott DJ, Heitzeg MM, Koeppe RA, Stohler CS, Zubieta J-K. Variations in the Human Pain Stress Experience Mediated by Ventral and Dorsal Basal Ganglia Dopamine Activity. Journal of Neuroscience. 2006;26:10789–10795.
6. Martikainen IK, Nuechterlein EB, Pecina M, Love TM, Cummiford CM, Green CR, et al. Chronic Back Pain Is Associated with Alterations in Dopamine Neurotransmission in the Ventral Striatum. Journal of Neuroscience. 2015;35:9957–9965.
7. JaÈaÈskelaÈinen SK, Rinne JO, Forssell H, Tenovuo O, Kaasinen V, Sonninen P, et al. Role of the dopaminergic system in chronic pain ± a ¯uorodopa-PET study. 2001:4.
8. Wood PB, Patterson JC, Sunderland JJ, Tainter KH, Glabus MF, Lilien DL. Reduced Presynaptic Dopamine Activity in Fibromyalgia Syndrome Demonstrated With Positron Emission Tomography: A Pilot Study. The Journal of Pain. 2007;8:51–58.
9. Chudler EH, Dong WK. The role of the basal ganglia in nociception and pain. Pain. 1995;60:3–38.
10. Ossipov MH, Dussor GO, Porreca F. Central modulation of pain. Journal of Clinical Investigation. 2010;120:3779–3787.
11. Hipolito L, Wilson-Poe A, Campos-Jurado Y, Zhong E, Gonzalez-Romero J, Virag L, et al. Inflammatory Pain Promotes Increased Opioid Self-Administration: Role of Dysregulated Ventral Tegmental Area Opioid Receptors. Journal of Neuroscience. 2015;35:12217–12231.
12. Markovic T, Pedersen CE, Massaly N, Vachez YM, Ruyle B, Murphy CA, et al. Pain induces adaptations in ventral tegmental area dopamine neurons to drive anhedonia-like behavior. Nat Neurosci. 2021;24:1601–1613.
13. Taylor AMW, Castonguay A, Taylor AJ, Murphy NP, Ghogha A, Cook C, et al. Microglia Disrupt Mesolimbic Reward Circuitry in Chronic Pain. J Neurosci. 2015;35:8442–8450.
14. Thomas SA, Matsumoto AM, Palmiter RD. Noradrenaline is essential for mouse fetal development. Nature. 1995;374:643–646.
15. Zhou Q-Y, Quaife CJ, Palmiter RD. Targeted disruption of the tyrosine hydroxylase gene reveals that catecholamines are required for mouse fetal development. Nature. 1995;374:640–643.
16. Willemsen MA, Verbeek MM, Kamsteeg E-J, de Rijk-van Andel JF, Aeby A, Blau N, et al. Tyrosine hydroxylase deficiency: a treatable disorder of brain catecholamine biosynthesis. Brain. 2010;133:1810–1822.
17. Johnson ME, Salvatore MF, Maiolo SA, Bobrovskaya L. Tyrosine hydroxylase as a sentinel for central and peripheral tissue responses in Parkinson's progression: Evidence from clinical studies and neurotoxin models. Progress in Neurobiology. 2018;165–167:1–25.
18. Lenartowski R, Goc A. Epigenetic, transcriptional and posttranscriptional regulation of the tyrosine hydroxylase gene. Int j Dev Neurosci. 2011;29:873–883.
19. Hwang D. Selective loss of dopaminergic neurons in the substantia nigra of Pitx3-deficient aphakia mice. Molecular Brain Research. 2003;114:123–131.
20. van den Munckhof P. Pitx3 is required for motor activity and for survival of a subset of midbrain dopaminergic neurons. Development. 2003;130:2535–2542.
21. Le W, Zhang L, Xie W, Li S, Dani JA. Pitx3 deficiency produces decreased dopamine signaling and induces motor deficits in Pitx3(−/−) mice. Neurobiology of Aging. 2015;36:3314–3320.
22. Kittappa R, Chang WW, Awatramani RB, McKay RDG. The foxa2 Gene Controls the Birth and Spontaneous Degeneration of Dopamine Neurons in Old Age. PLoS Biology.

2007;5:e325.
23. Kadkhodaei B, Ito T, Joodmardi E, Mattsson B, Rouillard C, Carta M, et al. Nurr1 Is Required for Maintenance of Maturing and Adult Midbrain Dopamine Neurons. Journal of Neuroscience. 2009;29:15923–15932.
24. Reddy SDN, Rayala SK, Ohshiro K, Pakala SB, Kobori N, Dash P, et al. Multiple coregulatory control of tyrosine hydroxylase gene transcription. Proceedings of the National Academy of Sciences. 2011;108:4200–4205.
25. Alavian KN, Jeddi S, Naghipour SI, Nabili P, Licznerski P, Tierney TS. The lifelong maintenance of mesencephalic dopaminergic neurons by Nurr1 and engrailed. Journal of Biomedical Science. 2014;21:27.
26. Hong S, Cho Y-W, Yu L-R, Yu H, Veenstra TD, Ge K. Identification of JmjC domain-containing UTX and JMJD3 as histone H3 lysine 27 demethylases. Proceedings of the National Academy of Sciences. 2007;104:18439–18444.
27. Agger K, Cloos PAC, Christensen J, Pasini D, Rose S, Rappsilber J, et al. UTX and JMJD3 are histone H3K27 demethylases involved in HOX gene regulation and development. Nature. 2007;449:731–734.
28. Lan F, Bayliss PE, Rinn JL, Whetstine JR, Wang JK, Chen S, et al. A histone H3 lysine 27 demethylase regulates animal posterior development. Nature. 2007;449:689–694.
29. Kartikasari AER, Zhou JX, Kanji MS, Chan DN, Sinha A, Grapin-Botton A, et al. The histone demethylase Jmjd3 sequentially associates with the transcription factors Tbx3 and Eomes to drive endoderm differentiation. The EMBO Journal. 2013;32:1393–1408.
30. Ohtani K, Zhao C, Dobreva G, Manavski Y, Kluge B, Braun T, et al. Jmjd3 Controls Mesodermal and Cardiovascular Differentiation of Embryonic Stem Cells. Circ Res. 2013;113:856–862.
31. Jepsen K, Solum D, Zhou T, McEvilly RJ, Kim H-J, Glass CK, et al. SMRT-mediated repression of an H3K27 demethylase in progression from neural stem cell to neuron. Nature. 2007;450:415–419.
32. Burgold T, Spreafico F, De Santa F, Totaro MG, Prosperini E, Natoli G, et al. The Histone H3 Lysine 27-Specific Demethylase Jmjd3 Is Required for Neural Commitment. PLoS ONE. 2008;3:e3034.
33. Zhao W, Li Q, Ayers S, Gu Y, Shi Z, Zhu Q, et al. Jmjd3 Inhibits Reprogramming by Upregulating Expression of INK4a/Arf and Targeting PHF20 for Ubiquitination. Cell. 2013;152:1037–1050.
34. Sen GL, Webster DE, Barragan DI, Chang HY, Khavari PA. Control of differentiation in a self-renewing mammalian tissue by the histone demethylase JMJD3. Genes & Development. 2008;22:1865–1870.
35. De Santa F, Totaro MG, Prosperini E, Notarbartolo S, Testa G, Natoli G. The Histone H3 Lysine-27 Demethylase Jmjd3 Links Inflammation to Inhibition of Polycomb-Mediated Gene Silencing. Cell. 2007;130:1083–1094.
36. Li Q, Zou J, Wang M, Ding X, Chepelev I, Zhou X, et al. Critical role of histone demethylase Jmjd3 in the regulation of CD4+ T-cell differentiation. Nature Communications. 2014;5:5780.
37. Ntziachristos P, Tsirigos A, Welstead GG, Trimarchi T, Bakogianni S, Xu L, et al. Contrasting roles of histone 3 lysine 27 demethylases in acute lymphoblastic leukaemia. Nature. 2014;514:513–517.
38. Przanowski P, Dabrowski M, Ellert-Miklaszewska A, Kloss M, Mieczkowski J, Kaza B, et al. The signal transducers Stat1 and Stat3 and their novel target Jmjd3 drive the expression of inflammatory genes in microglia. J Mol Med. 2014;92:239–254.
39. Tang Y, Li T, Li J, Yang J, Liu H, Zhang XJ, et al. Jmjd3 is essential for the epigenetic modulation of microglia phenotypes in the immune pathogenesis of Parkinson's disease. Cell Death & Differentiation. 2014;21:369–380.
40. Agger K, Cloos PAC, Rudkjaer L, Williams K, Andersen G, Christensen J, et al. The H3K27me3 demethylase JMJD3 contributes to the activation of the INK4A-ARF locus in response to oncogene- and stress-induced senescence. Genes & Development. 2009;23:1171–1176.

41. Liu Z, Cao W, Xu L, Chen X, Zhan Y, Yang Q, et al. The histone H3 lysine-27 demethylase Jmjd3 plays a critical role in specific regulation of Th17 cell differentiation. Journal of Molecular Cell Biology. 2015;7:505–516.
42. Zhang F, Xu L, Xu L, Xu Q, Li D, Yang Y, et al. JMJD3 promotes chondrocyte proliferation and hypertrophy during endochondral bone formation in mice. Journal of Molecular Cell Biology. 2015;7:23–34.
43. Zhang F, Xu L, Xu L, Xu Q, Karsenty G, Chen CD. Histone demethylase JMJD3 is required for osteoblast differentiation in mice. Scientific Reports. 2015;5.
44. He X-B, Kim M, Kim S-Y, Yi S-H, Rhee Y-H, Kim T, et al. Vitamin C Facilitates Dopamine Neuron Differentiation in Fetal Midbrain Through TET1- and JMJD3-Dependent Epigenetic Control Manner: Epigenetic Control of mDA Neuron Development by VC. STEM CELLS. 2015;33:1320–1332.
45. Pu T, Mei Z, Zhang W, Liang W, Zhou X, Liang J, et al. An in vitro DNA phosphorothioate modification reaction. Mol Microbiol. 2020;113:452–463.
46. Sun W, Shi J, Hong J, Zhao G, Wang W, Zhang D, et al. Natural variation and underlying genetic loci of γ-oryzanol in Asian cultivated rice seeds. The Plant Genome. 2022. 27 June 2022. https://doi.org/10.1002/tpg2.20201.
47. Wang H, Heijnen CJ, van Velthoven CTJ, Willemen HLDM, Ishikawa Y, Zhang X, et al. Balancing GRK2 and EPAC1 levels prevents and relieves chronic pain. J Clin Invest. 2013;123:5023–5034.
48. Chaplan SR, Bach FW, Pogrel JW, Chung JM, Yaksh TL. Quantitative assessment of tactile allodynia in the rat paw. Journal of Neuroscience Methods. 1994;53:55–63.
49. Hargreaves K, Dubner R, Brown F, Flores C, Joris J. A new and sensitive method for measuring thermal nociception in cutaneous hyperalgesia. Pain. 1988;32:77–88.
50. Kruidenier L, Chung C, Cheng Z, Liddle J, Che K, Joberty G, et al. A selective jumonji H3K27 demethylase inhibitor modulates the proinflammatory macrophage response. Nature. 2012;488:404–408.
51. Shi C-Y, He X-B, Zhao C, Wang H-J. Luteoloside Exerts Analgesic Effect in a Complete Freund's Adjuvant-Induced Inflammatory Model via Inhibiting Interleukin-1β Expression and Macrophage/Microglia Activation. Front Pharmacol. 2020;11:1158.
52. Shiotsuki H, Yoshimi K, Shimo Y, Funayama M, Takamatsu Y, Ikeda K, et al. A rotarod test for evaluation of motor skill learning. Journal of Neuroscience Methods. 2010;189:180–185.
53. Liang B, Zhang L, Zhang Y, Werner CT, Beacher NJ, Denman AJ, et al. Striatal direct pathway neurons play leading roles in accelerating rotarod motor skill learning. IScience. 2022;25:104245.
54. Bohlen M, Cameron A, Metten P, Crabbe JC, Wahlsten D. Calibration of rotational acceleration for the rotarod test of rodent motor coordination. Journal of Neuroscience Methods. 2009;178:10–14.
55. Chagniel L, Robitaille C, Lacharité-Mueller C, Bureau G, Cyr M. Partial dopamine depletion in MPTP-treated mice differentially altered motor skill learning and action control. Behavioural Brain Research. 2012;228:9–15.
56. Shoji H, Takao K, Hattori S, Miyakawa T. Age-related changes in behavior in C57BL/6J mice from young adulthood to middle age. Molecular Brain. 2016;9.
57. He X-B, Yi S-H, Rhee Y-H, Kim H, Han Y-M, Lee S-H, et al. Prolonged Membrane Depolarization Enhances Midbrain Dopamine Neuron Differentiation via Epigenetic Histone Modifications. STEM CELLS. 2011;29:1861–1873.
58. Yi S-H, He X-B, Rhee Y-H, Park C-H, Takizawa T, Nakashima K, et al. Foxa2 acts as a co-activator potentiating expression of the Nurr1-induced DA phenotype via epigenetic regulation. Development. 2014;141:761–772.
59. Hu Z, Cooper M, Crockett DP, Zhou R. Differentiation of the midbrain dopaminergic pathways during mouse development. J Comp Neurol. 2004;476:301–311.
60. La Manno G, Gyllborg D, Codeluppi S, Nishimura K, Salto C, Zeisel A, et al. Molecular Diversity of Midbrain Development in Mouse, Human, and Stem Cells. Cell. 2016;167:566-

580.e19.
61. Crawford GD, Le WD, Smith RG, Xie WJ, Stefani E, Appel SH. A novel N18TG2 x mesencephalon cell hybrid expresses properties that suggest a dopaminergic cell line of substantia nigra origin. Journal of Neuroscience. 1992;12:3392–3398.
62. Meredith GE, Sonsalla PK, Chesselet M-F. Animal models of Parkinson's disease progression. Acta Neuropathol. 2008;115:385–398.
63. Watabe-Uchida M, Zhu L, Ogawa SK, Vamanrao A, Uchida N. Whole-Brain Mapping of Direct Inputs to Midbrain Dopamine Neurons. Neuron. 2012;74:858–873.
64. Krabbe S, Duda J, Schiemann J, Poetschke C, Schneider G, Kandel ER, et al. Increased dopamine D2 receptor activity in the striatum alters the firing pattern of dopamine neurons in the ventral tegmental area. Proc Natl Acad Sci USA. 2015;112.
65. Huang S, Zhang Z, Gambeta E, Xu SC, Thomas C, Godfrey N, et al. Dopamine Inputs from the Ventral Tegmental Area into the Medial Prefrontal Cortex Modulate Neuropathic Pain-Associated Behaviors in Mice. Cell Reports. 2020;31:107812.
66. Vergara F, Sardi NF, Pescador AC, Guaita GO, Jark Stern CA, Chichorro JG, et al. Contribution of mesolimbic dopamine and kappa opioid systems to the transition from acute to chronic pain. Neuropharmacology. 2020;178:108226.
67. Wakaizumi K, Kondo T, Hamada Y, Narita M, Kawabe R, Narita H, et al. Involvement of mesolimbic dopaminergic network in neuropathic pain relief by treadmill exercise: A study for specific neural control with Gi-DREADD in mice. Mol Pain. 2016;12:174480691668156.
68. Taylor AMW, Murphy NP, Evans CJ, Cahill CM. Correlation Between Ventral Striatal Catecholamine Content and Nociceptive Thresholds in Neuropathic Mice. The Journal of Pain. 2014;15:878–885.
69. Dieb W, Ouachikh O, Durif F, Hafidi A. Nigrostriatal dopaminergic depletion produces orofacial static mechanical allodynia. Eur J Pain. 2016;20:196–205.
70. Hnasko TS, Sotak BN, Palmiter RD. Morphine reward in dopamine-deficient mice. Nature. 2005;438:854–857.
71. Zhang L, Wang J, Niu C, Zhang Y, Zhu T, Huang D, et al. Activation of parabrachial nucleus - ventral tegmental area pathway underlies the comorbid depression in chronic neuropathic pain in mice. Cell Reports. 2021;37:109936.
72. Sagheddu C, Aroni S, De Felice M, Lecca S, Luchicchi A, Melis M, et al. Enhanced serotonin and mesolimbic dopamine transmissions in a rat model of neuropathic pain. Neuropharmacology. 2015;97:383–393.
73. Sugiyama E, Kondo T, Kuzumaki N, Honda K, Yamanaka A, Narita M, et al. Mechanical allodynia induced by optogenetic sensory nerve excitation activates dopamine signaling and metabolism in medial nucleus accumbens. Neurochemistry International. 2019;129:104494.
74. Sun G-L, Song Z-J, Peng X-H, Chen P-P, Song Y, Qin X, et al. Projection-specific dopamine neurons in the ventral tegmental area participated in morphine-induced hyperalgesia and anti-nociceptive tolerance in male mice. J Psychopharmacol. 2021;35:591–605.
75. Watanabe M, Narita M, Hamada Y, Yamashita A, Tamura H, Ikegami D, et al. Activation of ventral tegmental area dopaminergic neurons reverses pathological allodynia resulting from nerve injury or bone cancer. Mol Pain. 2018;14:174480691875640.
76. Sagheddu C, Aroni S, De Felice M, Lecca S, Luchicchi A, Melis M, et al. Enhanced serotonin and mesolimbic dopamine transmissions in a rat model of neuropathic pain. Neuropharmacology. 2015;97:383–393.
77. Zhang H, Qian Y-L, Li C, Liu D, Wang L, Wang X-Y, et al. Brain-Derived Neurotrophic Factor in the Mesolimbic Reward Circuitry Mediates Nociception in Chronic Neuropathic Pain. Biological Psychiatry. 2017;82:608–618.
78. Brumovsky PR. Dorsal root ganglion neurons and tyrosine hydroxylase—an intriguing association with implications for sensation and pain: PAIN. 2016;157:314–320.
79. Seal RP, Wang X, Guan Y, Raja SN, Woodbury CJ, Basbaum AI, et al. Injury-induced mechanical hypersensitivity requires C-low threshold mechanoreceptors. Nature. 2009;462:651–655.

80. Puopolo M. The hypothalamic-spinal dopaminergic system: a target for pain modulation. Neural Regen Res. 2019;14:925.
81. Hashizume R, Andor N, Ihara Y, Lerner R, Gan H, Chen X, et al. Pharmacologic inhibition of histone demethylation as a therapy for pediatric brainstem glioma. Nature Medicine. 2014;20:1394–1396.
82. Lochmann TL, Powell KM, Ham J, Floros KV, Heisey DAR, Kurupi RIJ, et al. Targeted inhibition of histone H3K27 demethylation is effective in high-risk neuroblastoma. Sci Transl Med. 2018;10:eaao4680.

Figure legends

Figure 1. The effect of JMJD3 inhibition on levels of dopamine (DA), norepinephrine (NE) and serotonin (5-HT) in adult male mouse brain. Five brain regions are separately measured including frontal cortex (CTX), striatum (STRM), midbrain (MB), cerebellum (CB) and medulla oblongata (MO) by high performance liquid chromatography-mass spectrometry analysis. (A-C) DA, NE and 5-HT levels in different brain regions of mice underwent 5 days of intraperitoneal injection of JMJD3 inhibitor GSK-J4. (D-F) DA, NE and 5-HT levels from different brain regions in DA neuron-specific conditional knockdown mice (TH-KD) and their control littermates (TH-CRE). N = 4-7 mice. Data represent mean ± S.E.M. Red star represents $*P < 0.05$, Student's t-test.

Figure 2. DA neuron-specific JMJD3 knockdown inhibits TH expression in ventral tegmental area (VTA) but not substantia nigra pars compacta (SNpc) in vivo. (A) Real-time PCR analysis of mRNA levels of JMJD3 and TH from different brain regions in DA neuron-specific conditional knockdown mice (TH-KD) and their control littermates (TH-CRE). Note that both genes are specifically down-regulated in striatum (STRM) and midbrain (MB), but not frontal cortex (CTX), cerebellum (CB) or medulla oblongata (MO). N = 3 mice. Data represent mean ± S.E.M. (B) Representative immunofluorescence images showing TH-immunoreactive DA neurons in VTA and SNpc of TH-CRE and TH-KD mice. Scale bar represents 100 μm. (C, D) Quantification of TH immunoreactive intensity (C) and cell number (D) of DA neurons in VTA and SNpc in TH-CRE and TH-KD mice. At least 50 TH-expressing cells were measured and the mean was calculated for one mouse. N = 3-5 mice. Data represent mean ± S.E.M. $*P < 0.05$, $**P < 0.01$; Student's t-test.

Figure 3. DA neuron-specific JMJD3 knockdown affects mechanical hyperalgesia but not locomotor functions. (A-D) Effect of TH-specific JMJD3 knockdown on mechanical hyperalgesia in Complete Freund's adjuvant (CFA)-induced chronic inflammatory pain in young (A, B) and old (C, D), male (A, C) and female (B, D) heterozygous transgenic mice (TH-KD) and their control littermates (TH-CRE). Von Frey hairs test was performed at 3, 6h and day 1, 3, 8, 13, 18 after intraplantar CFA. Changes in 50% paw withdrawal threshold were calculated. (E-H)

Effect of TH-specific JMJD3 knockdown on locomotor coordination and motor skill learning in young (E, F) and old (G, H), male (E, G) and female (F, H) TH-KD and TH-CRE mice.The accelerating rotarod test indicating locomotor coordination of young TH-CRE and TH-KD male and female mice. (G-H) The accelerating rotarod test indicating locomotor coordination of old TH-CRE and TH-KD male and female mice. Data represent mean ± S.E.M. $*P < 0.05$, $**P < 0.01$, $****P < 0.0001$; two-way ANOVA with Sidak's multiple comparisons test.

Figure 4. JMJD3 directly transactivates TH gene expression. (A) Representative immunofluorescence images of TH-expressing DA neurons and cell number quantification in primary mouse DA neuronal cell culture with or without treatment of JMJD3 inhibitor GSK-J4. Cell numbers were counted in 10 random areas of each culture coverslip using an eyepiece grid at a magnification ×100. Scale bar represents 100 μm. (B) Real-time PCR analysis (qPCR) of TH mRNA expression after GSK-J4 treatment. (C) The quantification of TH+ cell number in primary mouse DA neuronal cell culture underwent short hairpin RNA-mediated JMJD3 knockdown (sh-JMJD3) or control (plko.1). (D) qPCR analysis of JMJD3, UTX and TH gene expressions after sh-JMJD3 knockdown. (E) Chromatin immunoprecipitation (ChIP)-qPCR analysis of histone 3 lysine 27 tri-methylation (H3K27me3) on 1 kilo bp mouse *Th* promoter region from primary DA neuronal cell samples with or without GSK-J4 treatment. (F) ChIP-qPCR analysis showing GSK-J4 altered region-specific JMJD3 enrichment on mouse *Th* promoter. N = 3 independent cell cultures. Data represent mean ± S.E.M. $*P < 0.05$; Student's t-test and one-way ANOVA with Tukey's post hoc test.

Supplemental Figure Legends

Supplemental Figure 1. Genotyping of TH-specific JMJD3 knockdown mice. Genetic DNAs were extracted from tails of mice and applied to semi-quantitative PCR analysis to verify the loci carrying CRE and JMJD3 loxP sequences using specific primers. Mice carrying one band by CRE primer and two bands by loxP primer represent heterozygous genotype (TH-KD) and mice carrying one band by CRE primer and one band near 300 bp by loxP primer represent control genotype (TH-CRE).

Supplemental Figure 2. The effect of JMJD3 knockdown on levels of dopamine (DA), norepinephrine (NE) and serotonin (5-HT) in adult female mouse brain. Five brain regions including frontal cortex (CTX), striatum (STRM), midbrain (MB), cerebellum (CB) and medulla oblongata (MO) in DA neuron-specific conditional knockdown female mice (TH-KD) and their control littermates (TH-CRE) were separately extracted, and the levels of DA (A), NE (B) and 5-HT (C) were measured by high performance liquid chromatography-mass spectrometry analysis. N = 4-7 mice. Data represent mean ± S.E.M. Red star represents $*P < 0.05$, Student's t-test.

Supplemental Figure 3. DA neuron-specific JMJD3 knockdown does not affect thermal hyperalgesia or grip strength. (A) Effect of TH-specific JMJD3 knockdown on thermal hyperalgesia in different age and sex TH-KD mice and TH-CRE mice by the Hargreaves method. Latencies of hind paw withdrawal were recorded. (B) Effect of TH-specific JMJD3 knockdown on grip strength in different age and sex TH-KD mice and TH-CRE mice. Data represent mean ± S.E.M., Student's t-test.

Supplemental Figure 4. Effect of GSK-J4 on TH expression in MES23.5 dopamine (DA) cell line. (A, B) Representative immunofluorescence images and quantification of TH-expressing cells in MES23.5 DA neuronal cell culture with or without treatment of JMJD3 inhibitor GSK-J4. Cell numbers were counted in 10 random areas of each culture coverslip using an eyepiece grid at a magnification ×100. Scale bar represents 100 μm. (C) Real-time PCR analysis of TH mRNA expression in response to different doses of GSK-J4 treatment. N = 3 independent cell cultures.

Data represent mean ± S.E.M. *$P < 0.05$; one-way ANOVA with Tukey's post hoc test.

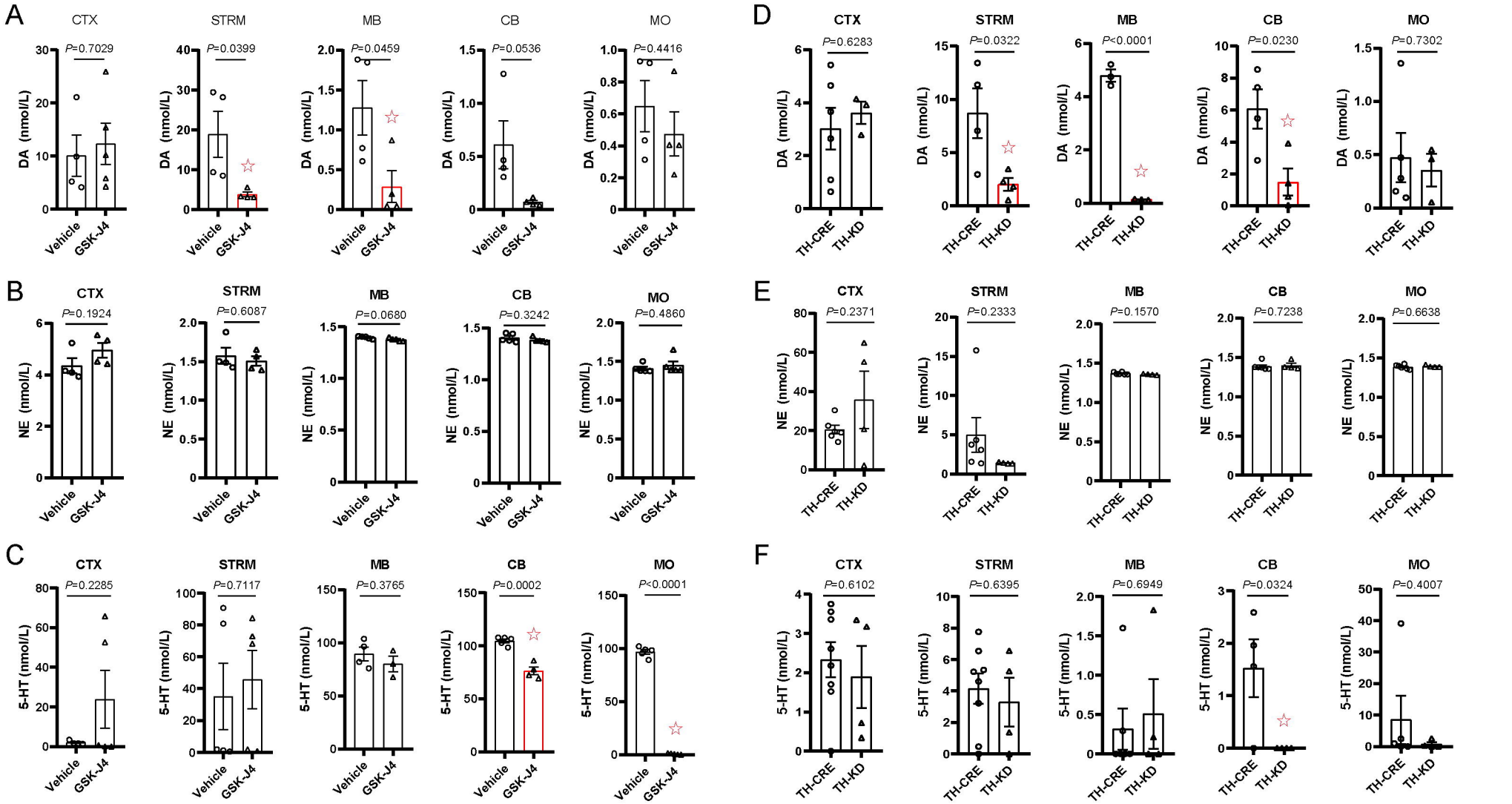
A
CTX
STRM
MB
CB
MO
P=0.7029
P=0.0399
P=0.0459
P=0.0536
P=0.4416
DA (nmol/L)
Vehicle
GSK-J4
B
P=0.1924
P=0.6087
P=0.0680
P=0.3242
P=0.4860
NE (nmol/L)
C
P=0.2285
P=0.7117
P=0.3765
P=0.0002
P<0.0001
5-HT (nmol/L)
D
P=0.6283
P=0.0322
P<0.0001
P=0.0230
P=0.7302
TH-CRE
TH-KD
E
P=0.2371
P=0.2333
P=0.1570
P=0.7238
P=0.6638
F
P=0.6102
P=0.6395
P=0.6949
P=0.0324
P=0.4007

A

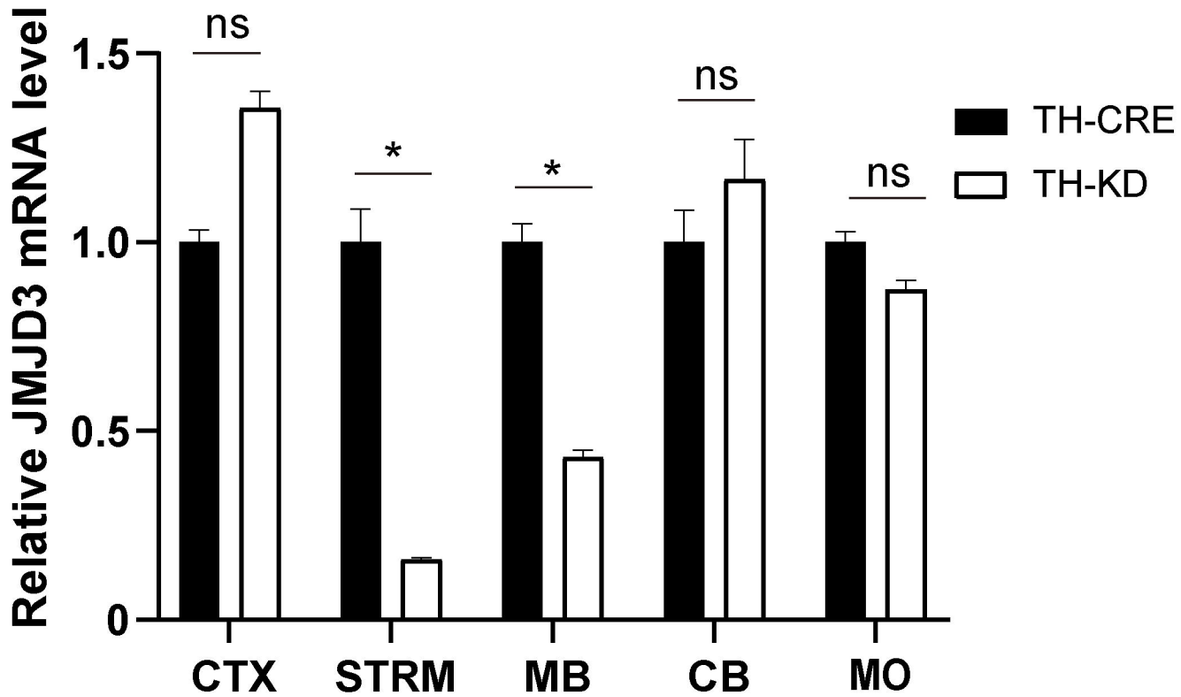
Relative JMJD3 mRNA level
1.5
1.0
0.5
0
ns
*
*
ns
ns
TH-CRE
TH-KD
CTX
STRM
MB
CB
MO

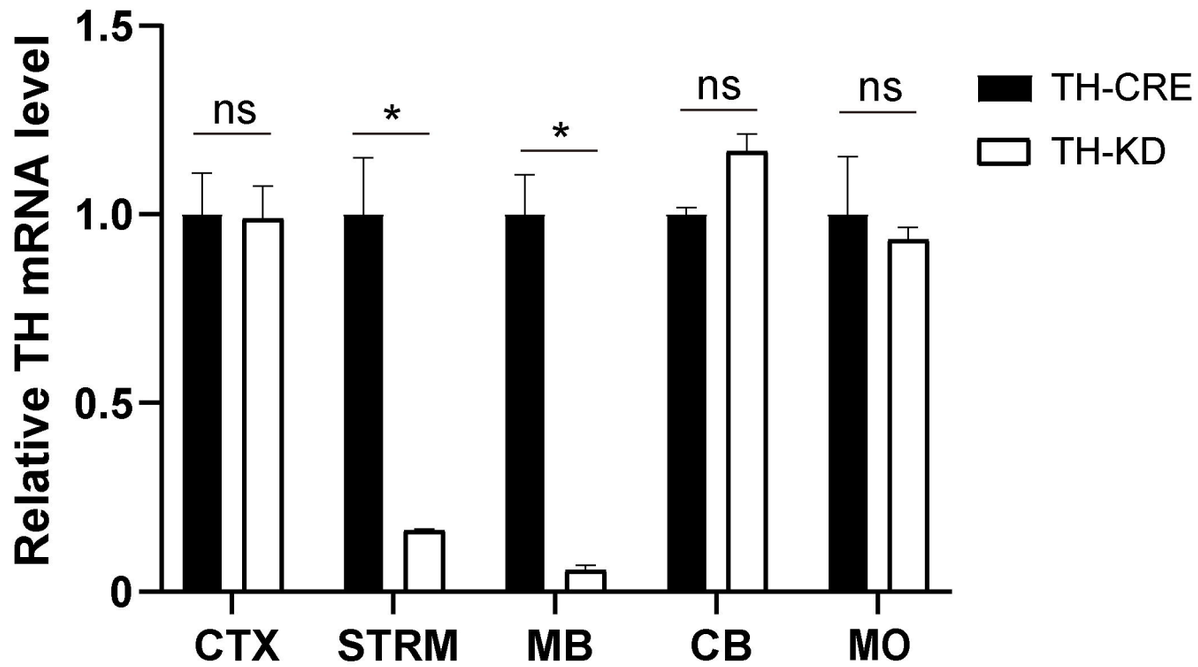
Relative TH mRNA level
1.5
1.0
0.5
0
ns
*
*
ns
ns
TH-CRE
TH-KD
CTX
STRM
MB
CB
MO

B

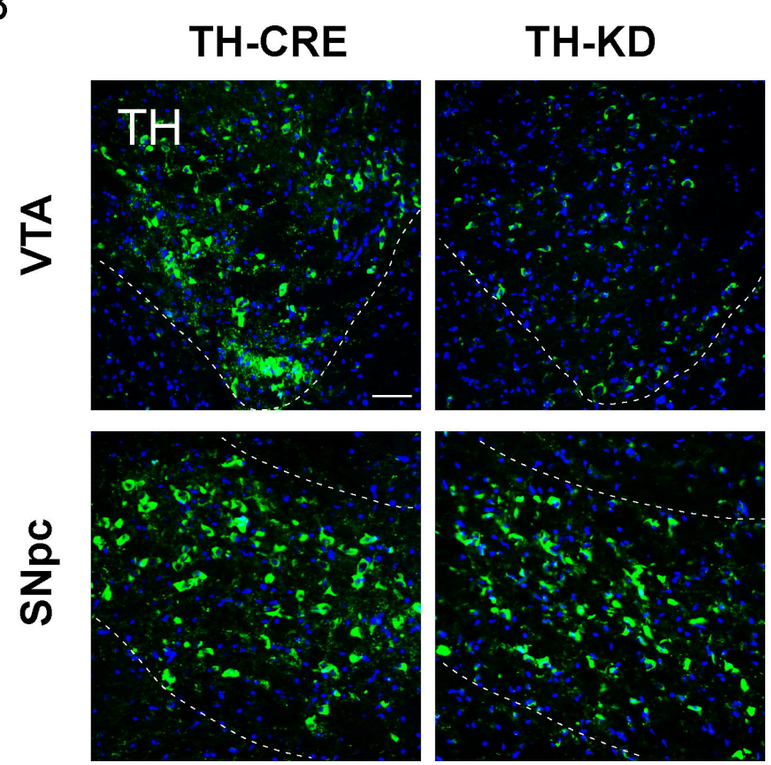
TH-CRE
TH-KD
TH
VTA
SNpc

C

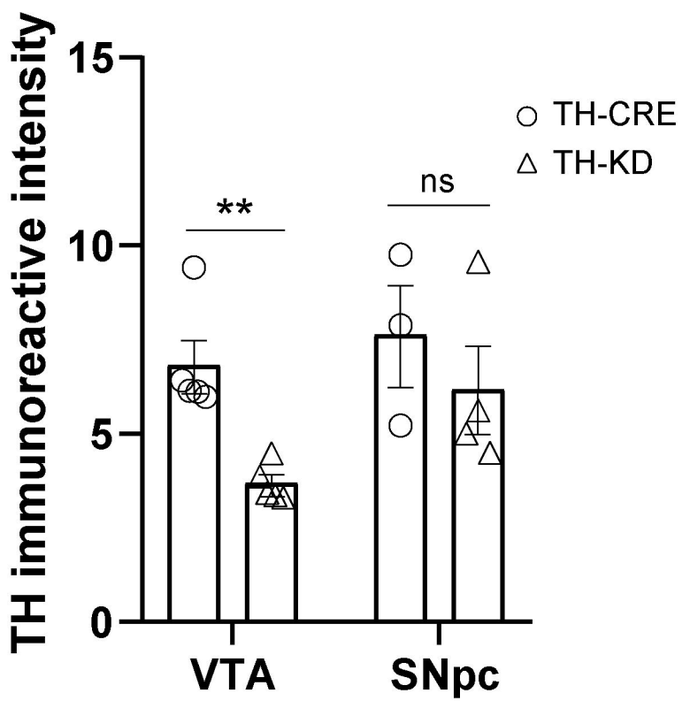
TH immunoreactive intensity
15
10
5
0
**
ns
TH-CRE
TH-KD
VTA
SNpc

D

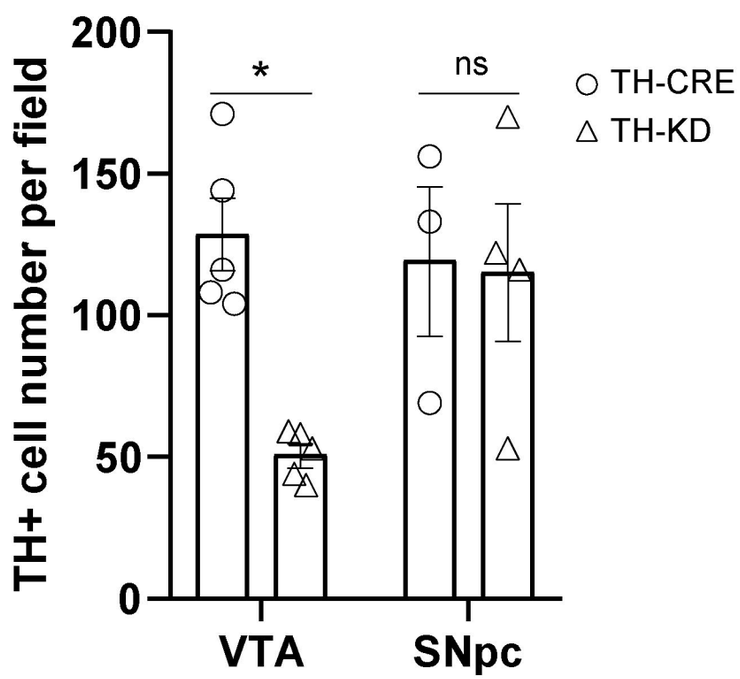
TH+ cell number per field
200
150
100
50
0
*
ns
TH-CRE
TH-KD
VTA
SNpc

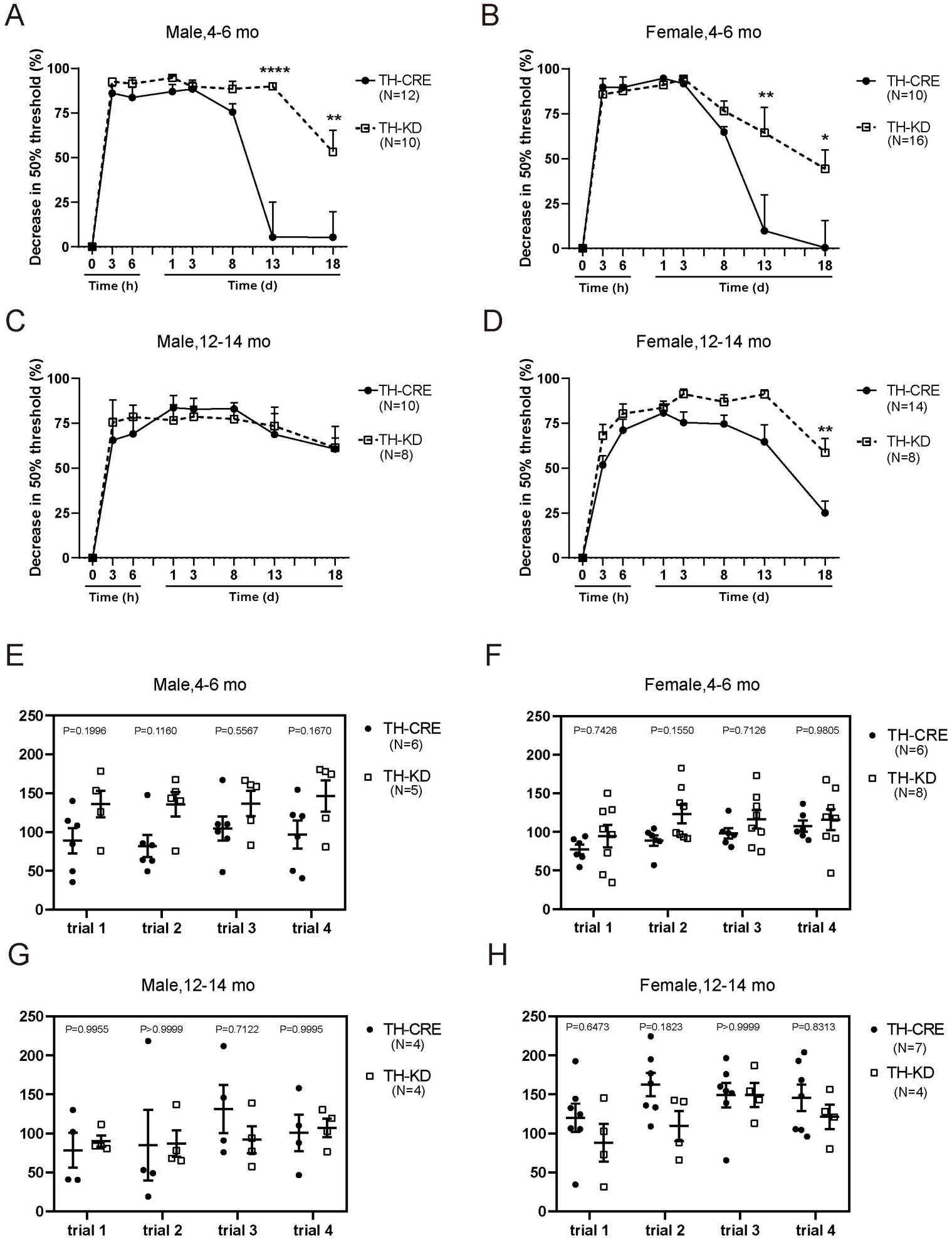
A
Male,4-6 mo
Decrease in 50% threshold (%)
100
75
50
25
0
****
**
TH-CRE
(N=12)
TH-KD
(N=10)
0 3 6
1 3 8 13 18
Time (h)
Time (d)
B
Female,4-6 mo
Decrease in 50% threshold (%)
**
*
TH-CRE
(N=10)
TH-KD
(N=16)
Time (h)
Time (d)
C
Male,12-14 mo
Decrease in 50% threshold (%)
TH-CRE
(N=10)
TH-KD
(N=8)
Time (h)
Time (d)
D
Female,12-14 mo
Decrease in 50% threshold (%)
**
TH-CRE
(N=14)
TH-KD
(N=8)
Time (h)
Time (d)
E
Male,4-6 mo
250
200
150
100
50
0
P=0.1996
P=0.1160
P=0.5567
P=0.1670
TH-CRE
(N=6)
TH-KD
(N=5)
trial 1
trial 2
trial 3
trial 4
F
Female,4-6 mo
P=0.7426
P=0.1550
P=0.7126
P=0.9805
TH-CRE
(N=6)
TH-KD
(N=8)
trial 1
trial 2
trial 3
trial 4
G
Male,12-14 mo
P=0.9955
P>0.9999
P=0.7122
P=0.9995
TH-CRE
(N=4)
TH-KD
(N=4)
trial 1
trial 2
trial 3
trial 4
H
Female,12-14 mo
P=0.6473
P=0.1823
P>0.9999
P=0.8313
TH-CRE
(N=7)
TH-KD
(N=4)
trial 1
trial 2
trial 3
trial 4

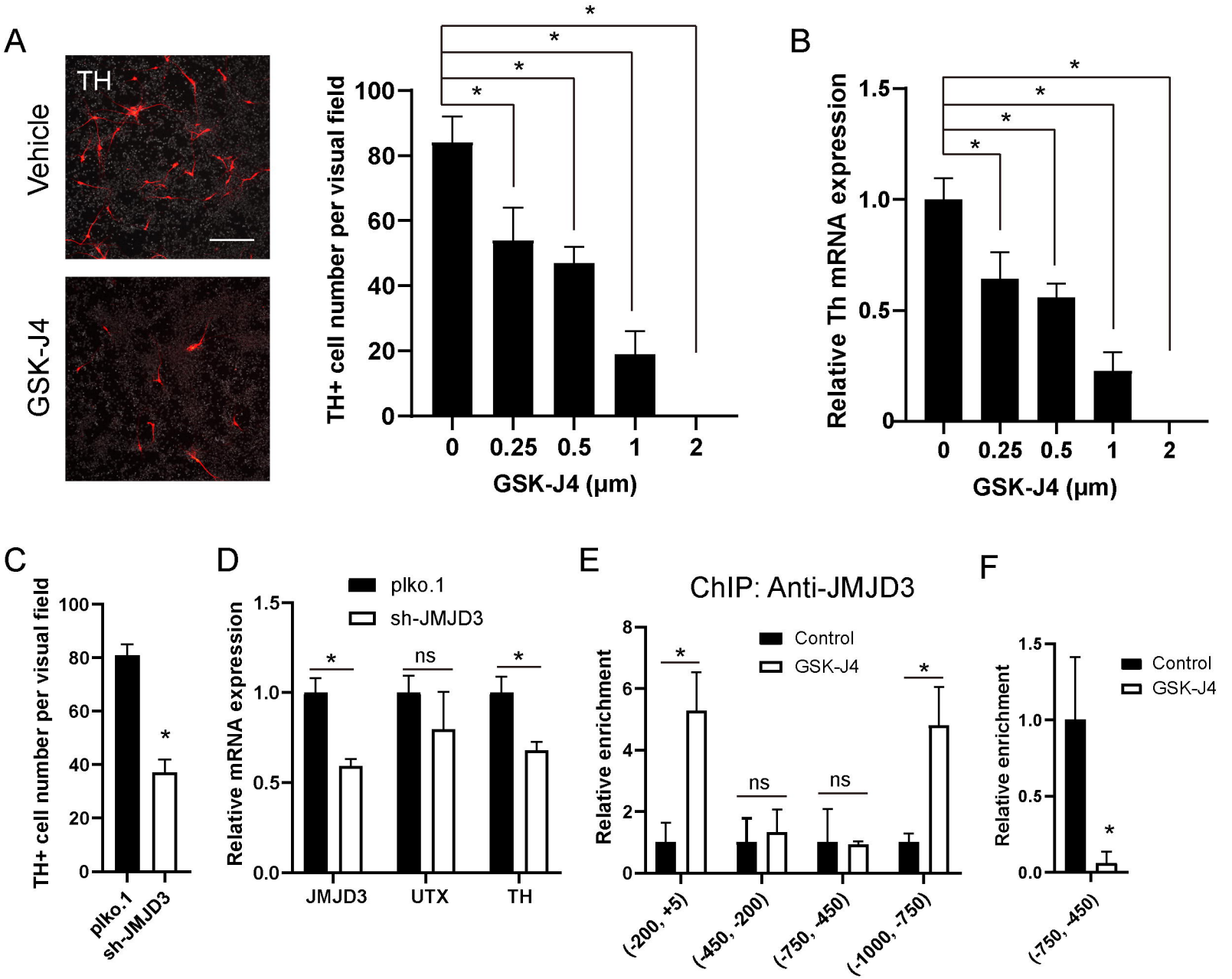
A
TH
Vehicle
GSK-J4
TH+ cell number per visual field
GSK-J4 (μm)
B
Relative Th mRNA expression
GSK-J4 (μm)
C
TH+ cell number per visual field
plko.1
sh-JMJD3
D
plko.1
sh-JMJD3
Relative mRNA expression
JMJD3
UTX
TH
ns
E
ChIP: Anti-JMJD3
Control
GSK-J4
Relative enrichment
(-200, +5)
(-450, -200)
(-750, -450)
(-1000, -750)
F
Control
GSK-J4
Relative enrichment
(-750, -450)